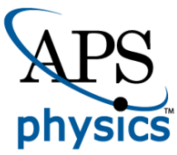

New Ground-State Crystal Structure of Elemental Boron

Qi An, K. Madhav Reddy, Kelvin Y. Xie, Kevin J. Hemker, and William A. Goddard, III

Phys. Rev. Lett. **117**, 085501 — Published 15 August 2016

DOI: 10.1103/PhysRevLett.117.085501

New Ground State Crystal Structure of Elemental Boron

Qi An,[1+] Madhav Reddy,[2+] Kelvin. Y. Xie[2], Kevin J. Hemker,[2*] and William A. Goddard III[1*]

[1]*Materials and Process Simulation Center,*

California Institute of Technology, Pasadena, CA 91125, USA

[2]*Department of Mechanical Engineering, Johns Hopkins University, Baltimore, MD 21210, USA*

[+]These authors contributed equally to this work.

[*]Corresponding author E-mail: hemker@jhu.edu, wag@wag.caltech.edu,

Abstract: Elemental boron exhibits many polymorphs in nature based mostly on an icosahedral shell motif, involving stabilization of 13 strong multicenter intra-icosahedral bonds. It is commonly accepted that the most thermodynamic stable structure of elemental boron at atmospheric pressure is the β rhombohedral boron (β-B). Surprisingly, using high-resolution transmission electron microscopy (HRTEM), we found that pure boron powder contains grains of two different types, the previously identified β-B containing a number of randomly spaced twins and what appears to be a fully transformed twin-like structure. This fully transformed structure, denoted here as τ-B, is based on the *Cmcm* orthorhombic space group. QM predicts that the newly identified τ-B structure is 13.8 meV/B *more stable* than β-B. The τ-B structure allows 6% more charge transfer from B_{57} units to nearby B_{12} units, making the net charge 6% closer to the ideal expected from Wade's rules. Thus, we predict the τ-B structure to be the ground state structure for elemental boron at atmospheric pressure.

Boron and related materials exhibit such extreme properties as low density, high hardness, high melting temperature, superconductivity, and ferromagnetism [1−14], making them candidates for such applications as high power electronics, superconductors, heat resistant alloys, coatings in nuclear reactors, body armor vests, abrasives, and cutting tool applications [7−17]. However, boron leads to quite complex structures arising from its unique bonding character that prefers formation of icosahedral shell complexes that stabilize 13 strong multicenter intra-icosahedral bonds (requiring 26 electrons, Wade's rule). These complex structures make it difficult to interpret and understand the relationships between structure and properties. Indeed, even the ground state structure of boron has been controversial for over 30 years [6, 15−17].

A number of crystalline structural forms for elemental boron have been discovered over the last two centuries [18−20]. However, only three phases correspond to pure boron: α-B_{12} [18], β-B_{105} [19], and γ-B_{28} [20], with most of the others probably stabilized by impurities [21−23]. It has been long suspected that the β rhombohedral boron (β-B_{105}) structure is the most thermodynamic stable allotrope at low pressures [6,15−17]. However, the QM studies [15,16] predict that the α-B_{12} structure is more stable than β-B_{105} by 25.3 meV/atom, leading to a long debate of which phase is the ground state structure for elemental boron [6,15−17,24]. Recent QM studies have suggested that particular choices for the partial occupation sites in β-B_{105} and including zero point motion might lead to an energy for β-B_{105} that is more stable than α-B_{12} structure at ambient conditions [16,25].

Twinned structures have been observed in β-B_{105} [26,27] and boron related materials such as B_4C [28]. Although the growth conditions to form these twinned structures are not clear [27,29], the twinned structure might dramatically change material properties such as charge capacitance [30]. In this light, understanding the twinned structure in β-B_{105} and the other icosahedral based materials provides essential information for understanding material behaviors at realistic conditions.

Herein, we report HRTEM on high purity boron that shows two phases:

(1) About two thirds of the representative grains correspond to the well-known β rhombohedral

boron (β-B) structure (see Fig. S1 of Supplementary Materials (SM) [31]). These grains all contained a significant number of well-separated and randomly spaced twins.

(2) The other one third of the grains displays a perfectly ordered zig-zag "twin-like" atomic structure that extends across the entire grain.

In order to understand the nature of fully transformed grains, we constructed a model for the zig-zag structure and used QM to optimize it, leading to a *Cmcm* structure, denoted as τ-B with ordered twins that exactly match the HRTEM. Most interesting is that the QM finds this τ-B structure to be *more stable* than β-B by 13.8 meV/B and more stable than α-B_{12} by 9.5 meV/B. Moreover XRD analysis of boron powders containing the fully transformed grains agrees with the predicted τ-B structure. Combining these experimental and QM results we conclude that **the τ-B structure is the true ground state structure for elemental boron.**

The original β-B (denoted β-B_{105}) structure proposed by Hoard in 1970 [32] consists 105 atoms with 15 nonequivalent boron positions (B1 to B15) in the unit cell, which is well described in previous literature [33]. The unit cell of β-B_{105} consists of 8 icosahedral clusters at the vertex sites and 12 icosahedral clusters at the edge centers in the rhombohedral unit cell, as shown in Fig. 1(a). In addition, the single B15 atom is located in the cell center connecting to two B_{28} units (each of which consists of three partial icosahedral clusters) through B13 sites along the $[111]_r$ direction as shown in Fig. 1(b). The β-B_{105} structure has space group $R\bar{3}m$. Later, the β-B_{105} structure was refined experimentally [34] and determined to contain 320 atoms in the hexagonal unit cell with 5 additional partially occupied sites (POS). The most occupied of these POS, are B13 (74.5% occupied) and B16 (27.2% occupied), as shown in Fig. 1(a) (the other POS sites have partial occupancies < 10% [34]). Since the hexagonal unit cell corresponding to the rhombohedral unit cell contains 320 = 3 × 106.67 atoms, the refined β-B_{105} structure was denoted as β-B_{106} in the recent literature [16,25,33].

In our QM simulations, we consider two β-B structures

- β-B_{105} which corresponds to the original structure without POS; the QM predicted structure leads to lattice parameters of a = 10.11 Å and α = 65.4° which agree very well with

experimental values [32] of a = 10.14 Å and α = 65.2°.

- β-B_{106} containing one B13 vacancy site and two B16 occupied sites (this leads to exactly 106 atoms / cell). This particular β-B_{106} structure is selected because previous QM calculation [16] showed it to be the lowest energy structure among the structures consistent with the POS. The QM predicted β-B_{106} structure leads to lattice parameters of a = 10.09 Å, b = 10.16 Å, c = 10.16 Å, α = 65.1°, β = 65.0°, and γ = 65.1°, which also agrees very well with experimental values.

The β-B_{106} structure is more stable than β-B_{105} structure by 24.2 meV/atom, which is consistent with previous QM simulations [16]. Thus, we conclude that the B_{106} description is a better assignment than β-B_{105} for the β-B structure and we will mainly discuss this phase from this point on. Our QM calculations for the fully minimized structures find β-B_{106} to be less stable than α-B_{12} phase by 1.1 meV/atom without considering zero point energy (ZPE) corrections [16]. We calculated the ZPEs using a finite difference method [16]. The ZPEs for α-B_{12} and β-B_{106} phases are 130.0 and 126.6 meV/B, respectively, which agrees very well with the values of 130 and 126 meV/B in the previous study [16]. Using ZPE corrections for these two phases, we find that β-B_{106} is more stable than α-B_{12} by 2.3 meV/B, which agrees very well with the value of 2.9 meV/B from a previous study [16]. Previous studies [16] did not consider London dispersion when comparing the stability of the α-B_{12} and β-B_{106} phases. Here we include the London dispersion as incorporated in the Grimme D3 correction [35]. Including the ZPE and dispersion corrections, we predicted that β-B_{106} is less stable than α-B_{12} phase by 4.3 meV/B and less stable than τ-B_{106} by 13.8 meV/B.

The commercial β-boron powder used in this study was procured from H. C. Starck (H.C. Starck GmbH, Germany, purity level > 99.2% (with MgO (<0.8%) as the main impurity). To determine the crystal structure of these powders, we performed X-ray diffraction analyses to obtain the pattern shown in Fig. 2 where the simulated XRD pattern computed based on the QM derived β-B_{106} structure is compared with experiment. Our experimental pattern contains additional peaks shown by red arrows in Fig. 2. The additional peaks could not be attributed to

impurities, and their presence suggested that the boron powder contained a new structure in addition to β-B.

To investigate the powder samples further, we performed HRTEM experiments on individual grains, as shown in Fig. 3(a). The chemical composition of individual particles was measured using electron energy loss spectroscopy (EELS) and confirmed to be pure boron (Fig. S2 of SM). The HRTEM images obtained from more than 20 individual grains find that 65% have the β-B crystal structure (Fig. S1 of SM), while 35% were observed to have a perfectly ordered zig-zag pattern with the icosahedra alignment alternating every other plane. Here we denote the new zig-zag structure as τ-B. We note here that our XRD peak intensities do not reproduce the ratio of β-B and τ-B grains that we characterized by TEM, and we attribute this to variations in grain morphology and the fact that we only observed 20 grains.

This zig-zag structure has a mirror symmetry across the (001) plane and appears to be a uniformly twinned version of β-B (Fig. 3(b) provides a view along the [010] direction). Where observed, this new zig-zag structure extends across the entire grain as can be seen from multiple zone axes (Fig S3 and Fig. S4 of SM). The observed HRTEM images (Fig. 3, Fig. S3 and Fig. S4) from multiple zone axes suggest that this new structure has a structure similar to β-B but with a plane of mirror symmetry at the $\{001\}_r$ edge of every unit cell. Such extensive ordering is most unusual; usually twinned structures exhibit multiple and highly variable crystalline layers between the twin boundaries. This suggested that the observed structure might be a new crystal structure.

To examine the nature of this unique "twin-like" structure using QM, we constructed and optimized with QM two unique "twin-like" structures (τ-B_{105} and τ-B_{106}) based on the β-B_{105} and β-B_{106} structures, respectively.

- The optimized τ-B_{105} belongs to the *Cmcm* orthorhombic space group, with primitive cell parameters of a = 10.10 Å, b = 10.10 Å, c = 17.56 Å and γ = 65.4°. The primitive unit cell (shown in Fig. 1(c)) contains 210 atoms, exactly twice that of β-B_{105}.
- The new τ-B_{106} structure belongs to the *P1* space group with cell parameters of a = 10.08 Å,

b = 10.17, c = 17.57, α = β = 90°, and γ = 65.2°, while its unit cell contains 212 atoms, exactly twice that of β-B_{106}. We calculate that the energy of τ-B_{106} is 12.4 meV lower than τ-B_{105}, so we conclude that τ-B_{106} is the more stable structure for the τ-B phase and we will focus on the τ-B_{106} model further and discuss the τ-B_{105} model only in the charge calculation.

We calculate that the energy of the τ-B_{106} structure is 13.8 meV/B lower than β-B_{106} and 12.7 meV/B lower than the α-B_{12} phase. The absolute QM energies and the cohesive energies are listed in Table S1 of SM. Since the τ-B is the unique twin-like structure of β-B, we assume that the ZPE correction to τ-B phase is the same as β-B. Thus, including ZPE and dispersion correction we expect that τ-B_{106} more stable than β-B_{106} by 13.8 meV and more stable than α-B_{12} by 9.5 meV. Thus τ-B_{106} is the ground state of elemental Boron.

To compare directly the experimentally discovered fully transformed and fully twinned grains with the new theoretically calculated τ-B structure, we simulated the X-ray and electron diffraction patterns and HRTEM images using the QM derived atomic positions of the τ-B structure. The comparison of experimental and simulated XRD is shown in Fig. 2. This new τ-B_{106} structure accounts for the missing peaks in the experimental XRD, as indicated by the red dashed lines in Fig. 2. The other peaks in the experimental XRD come from the β-B, as indicated by the dashed blue lines in Fig. 2. Thus, comparing the simulated and experimental XRD patterns indicates that the powder samples contain a mixture of β-B and τ-B structures.

Experimental and simulated selected area electron diffraction (SAED) patterns are compared in Fig. 3. The experimental TEM SAED (Fig. 3(d)) was obtained from the grain that is shown in Fig. 3(b), and the simulated SAED (Fig. 3(e)) is based on the QM derived τ-B structure, except that we have averaged over the POS since these would be randomly occupied in various regions to yield the full space group symmetry, *Cmcm*, of the τ-B_{105} structure. Viewed along the [010] zone axis, the τ-B structure looks like rhombohedral boron with twins present at every second lattice plane. The τ-B structure can also be represented with the unit cell shown in Fig. 3(f). The lattice spacings of the (100) and (001) planes are labeled as d_1 and d_2, and their corresponding distances in reciprocal space are noted in the SAED patterns in Figs. 3(d,e). These

experimental and simulated diffraction patterns index identically. Moreover, the experimentally measured ratio (d_2/d_1 = 1.90) agrees well with the geometry of the QM simulated τ-B_{106} structure, where $c/(a\times\sin(\gamma))$ = 1.92. The experiments found very lower intensity reflections marked by arrowheads which were found to be equally spaced along the (001) planes (Fig. 3(d) and Fig. 3(e)). We also note that the relative intensity of spots in SAED is highly dependent on foil thickness, precise orientation, etc. and precession electron diffraction might be required to obtain a better match.

Moreover, the close match between the experimental (Fig. 3(c)) and simulated (Fig. 3(f)) HRTEM images further confirms the presence of the τ-B_{106} structure in the B powders. In addition, experimental HRTEM images and Fourier transforms patterns (Fig. S3 and Fig. S4 of SM) obtained using grains that were oriented along different zone axes i.e., <010> and <110> support this observation and agree with our hypothesis that the experimentally observed new phase is the τ-B_{106} structure.

The calculated stability of the new τ-B structure relative to other boron polymorphs, (β-B_{106}, α-B_{12} and γ-B_{28}) is displayed in Table 1. We see that τ-B_{106} is more stable than α-B_{12} by 12.7 meV/atom, while other phases β-B_{106}, γ-B_{28} are higher in energy than α-B_{12} by 1.1, and 27.3 meV/atom, respectively, which is consistent with previous QM simulations [15,16]. Considering ZPE and dispersion corrections, τ-B_{106} is more stable than α-B_{12} by 9.5 meV/atom and more stable than β-B_{106} by 13.8 meV/atom.

The predicted density of τ-B_{106} is 2.326 g/cm^3, which is similar to predicted densities of 2.328 g/cm^3 for β-B_{106}, 2.476 g/cm^3 for α-B_{12}, and 2.566 g/cm^3 for γ-B_{28}. The bonding in β-B is complex making it difficult to understand why τ-B_{106} is more stable than β-B_{106} but the electron counting rules proved valuable in understanding other phases of boron [33,36] should apply equally to τ-B. To gain insight into why τ-B phase is more stable, we calculated the charge distributions of the B_{12} and B_{57} (B_{28}-B-B_{28}) units in the β-B_{105} and τ-B_{105} structures, as shown in Fig. S5 of SM. The electron counting rules in β-B_{105} imply that two electrons must be added to each B_{12} unit to satisfy Wade's rule while the B_{57} units should donate three electrons to satisfy

the mno rule [33]. The charge distributions in β-B_{105} show that the three B_{12} units in the edge center of rhombohedral unit cell have -0.464 charge and one B_{12} unit in the corner has -0.085 charge for a net transfer of 1.477 while the B_{57} units has a balancing charge of +1.477 charge. (The B_{57} units transfer more electrons to 3 edge center B_{12} units because the B_{28} unit in B_{57} is closer to these three B_{12} units (~6.1 Å) than the one B_{12} in the corner (9.1 Å)) These changes are consistent with the electron counting rules but with smaller amounts than the idealized rules. In contrast, the B_{57} units in the τ-B_{105} structure transfers 1.566 electrons to the nearby B_{12} units, leading to -0.511, -0.511, -0.519 charges for three edge center B_{12} units and -0.025 for one corner B_{12} unit (a total of 1.566). Thus, τ-B_{105} leads to a 6% increase in the charge transferred to the τ-B_{105} units, making them closer to the electron counting rule [33], which may be why τ-B_{105} is more stable.

In summary, we discovered a new τ-B phase for elemental boron by combining XRD and HRTEM experiments with QM simulations. This new phase can be thought of as a perfectly ordered twin-like version of the original β-B structure, with a doubled unit cell. The QM studies indicate that this new phase is substantially more stable that either α-B_{12} or β-B, making it the true ground state structure of boron.

Acknowledgement

QA and WAG were supported by the Defense Advanced Research Projects Agency (W31P4Q-13-1-0010, program managers, John Paschkewitz), by the Army Research Laboratory under Cooperative Agreement Number W911NF-12-2-0022, and by the National Science Foundation (DMR-1436985, program manager, John Schlueter). KMR, KYX and KH were supported by the Defense Advanced Research Projects Agency (W31P4Q-13-1-0001). We gratefully acknowledge Prof. Richard Haber and Dr. Chawon Hwang at Rutgers University, for coordinating our access to the commercial boron powders. We thank ARL for permission to use their HRTEM simulation facility.

Author contributions

Q.A., K.M.R., K.H., and W.A.G. wrote the manuscript. K.M.R. performed the experimental measurements and image simulations including TEM and XRD, K.Y.X. contributed to the TEM, and Q.A. performed the QM simulations. Q.A., K.M.R., K.Y.X., K.H., and W.A.G. analyzed the data and discussed the results. K.M.R. first observed the new structure before Q.A. performed the QM simulations.

References

[1] D. A. Young, *Phase Diagrams of the Elements* (University of California Press, Berkeley, CA, 1991).

[2] J. L. Hoard and R. E. Hughes, *The Chemistry of Boron and Its Compounds* (Edited by Muetterties, E, L. Wiley, New York, 1967).

[3] B. Albert and H. Hillebrecht, Angew Chem. Int. Ed. **48**, 8640 (2009).

[4] Q. An, W. A. Goddard III, H. Xiao and T. Cheng, Chem. Mater. **26**, 4289 (2014).

[5] T. Ogitsu, E. Schwegler and G. Galli, Chem. Rev. **113**, 3425 (2013).

[6] M. A. White, A. B. Cerqueira, C. A. Whitman, M. B. Johnson and T. Ogitsu, Angew Chem. Int. Ed. **54**, 3626 (2015).

[7] E. Zarechnaya, *et. al.,* Phys. Rev. B **82**, 184111 (2010).

[8] D. N. Sanz, P. Loubeyre and M. Mezouar, Phys. Rev. Lett. **89**, 245501 (2002).

[9] M. Vlasse, R. Naslain, J. S. Kasper and K. Ploog, J. of Solid State Chem. **28**, 289 (1979).

[10] M. I. Eremets, V. V. Struzhkin, H-K. Mao and R. J. Hemley, Science **293**, 272 (2010).

[11] M. W. Chen, J. W. McCauley and K. J. Hemker, Science **299**, 1563 (2003).

[12] L. Schlapbach and A. Züttel, Nature **414**, 353 (2001).

[13] H. Zhang, Q. Zhang, J. Tang and L. C. Qin, J. Am. Chem. Soc. **127**, 2862 (2005).

[14] J. Nagamatsu, N. Nakagawa, T. Muranaka, Y. Zenitani and J. Akimitsu, Nature **410**, 63. (2010).

[15] S. L. Shang, Y. Wang, R. Arroyave and Z-K. Liu, Phys. Rev. B **75**, 092101 (2007).

[16] M. J. van Setten, M. A. Uijttewaal, G. A., de Wijs and R. A. de Groot, J. Am. Chem. Soc. **129**, 2458 (2007).

[17] L. V. McCarty, J. S. Kasper, F. H. Horn, B. F. Decker and A. E. Newkirk, J. Am. Chem. Soc. **80**, 2592 (1958).

[18] A. R. Oganov and V. L. Solozhenko, J. Superhard Mater. **31,** 285 (2009).

[19] R. E. Hughes, C. H. L. Kennard, D. B. Sullenger, H. A. Weakliem, D. Sands and J.

L. Hoard, J. Am. Chem. Soc. **85**, 361 (1963).

[20] A. R. Oganov, *et. al.*, Nature **457**, 863 (2009).

[21] R. H. Wentorf, Science **147**, 49 (1965).

[22] C.-Z. Fan, J. Li and L.-M. Wang, Scientific Reports **4**, 6786 (2014).

[23] R. E. Hughes, M. E. Leonowicz, J. T. Lemley and L.-T. Tai, J. Am. Chem. Soc. **99,** 5507 (1977).

[24] D. L. V. K. Prasad, M. M. Balakrishnarajan and E. D. Jemmis, Phys. ReV. B **72**, 195102, (2005).

[25] T. Ogitsu, F. Gygi, J. Reed, Y. Motome, E. Schwegler and G. Galli, J. Am. Chem. Soc. **131**, 1903 (2009).

[26] F. N. Tavadze, Ia Bairamas, Gv Tsagarei, K. P. Tsomaya and N. A. Zoidze, Sov. Phys. Crystal. USSR **9**, 768 (1965).

[27] G. S. Darsavelidze, O. A. Tsagareishvili, T. V. Eterashvili, V. S. Metreveli, G. F. Tavadze and D. I. Khomeriki, J. Less-Common Met. **117**, 189 (1986).

[28] K. Y. Xie, *et. al.*, Phys. Rev. Lett. **115**, 175501 (2015).

[29] M. E. Antadze, G. V. Tsagareishvili, O. A. Tsagareishvili, D. N. Tsikaridze and A. G. Khvedelidze, J. Less-Common Met. **117**, 153 (1986).

[30] O. A. Tsagareishvili, L. S. Chkhartishvili and D. L. Gabunia, Semicond. **43**, 14 (2009).

[31] See Supplemental Material, which includes Refs. [37–47], Figures S1-S6, Tables S1 The Supporting Materials include: (i) Experimental and Simulation details (ii) TEM characterization of β-B; (iii) Electron energy loss spectroscopy (EELS) analysis indicating that the grains studied were pure boron; (iv) TEM characterization of the newly observed τ-B phase along a <010> zone axis; (v) TEM characterization of newly observed τ-B phase along a <110> zone axis; (vi) Charge distributions (NBO analysis) of B_{12} and B_{57} units in β-B105 and τ-B105 structures; and (vii) the predicted structural parameters in Crystallographic Information File base format.

[32] J. L. Hoard, D. B. Sullenger, C. H. L. Kennard and R. E. Hughes, J. Solid State Chem. **1**, 268 (1970).

[33] E. D. Jemmis and M. M. Balakrishnarajan, J. Am. Chem. Soc. **123**, 4324 (2001).

[34] G. A. Slack, C. I. Hejna, M. F. Garbauskas and J. S. Kasper, J. Solid State Chem. **76**, 52−63 (1988).

[35] S. Grimme, J. Antony, S. Ehrlich, and S. Krieg, J. Chem. Phys. **132**, 154104 (2010).

[36] D. M. P. Mingos, Nat. Phys. Sci. **236**, 99 (1972).

[37] G. Kresse and J. Hafner, Phys. Rev. B **47**, 558 (1993).

[38] G. Kresse and J. Furthmuller, Comput. Mater. Sci. **6**, 15 (1996).

[39] G. Kresse and J. Furthmu□ller, Phys. Rev. B **16**, 11169 (1996).

[40] G. Kresse and D. Joubert, Phys. Rev. B **59**, 1758 (1999).

[41] B. D. Dunnington and J. R. Schmidt, J. Chem. Theory. Comput. **8**, 1902 (2012).

[42] K. Ishizuka and N. Uyeda, Acta Cryst. **33**, 740 (1977).

[43] O. O. Kurakevch and V. L. Solozhenko, Acta. Cryst. **63**, i80 (2007).

[44] R. E. Hughes, C. H. Kennard, D. B. Sullenger, H. A. Weakliem, D. E. Sands and J. L. Hoard, J. Am. Chem. Soc. **85**, 361 (1963).

[45] J. L. Hoard, D. B. Sullenger, C. H. L. Kennard and R. E. Hughes, J. Solid State Chem. **1**, 268 (1970).

[46] M. J. McKelvy, A. R. Rae Smith, and L. Eyring, J. Solid State Chem. **44**, 374 (1982).

[47] P. Favia, T. Stoto, M. Carrard, P. A. Stadelmann, and L. Zuppiroli, Microsc. Microanaly. Microstruct. **7**, 225 (1996).

Figure 1

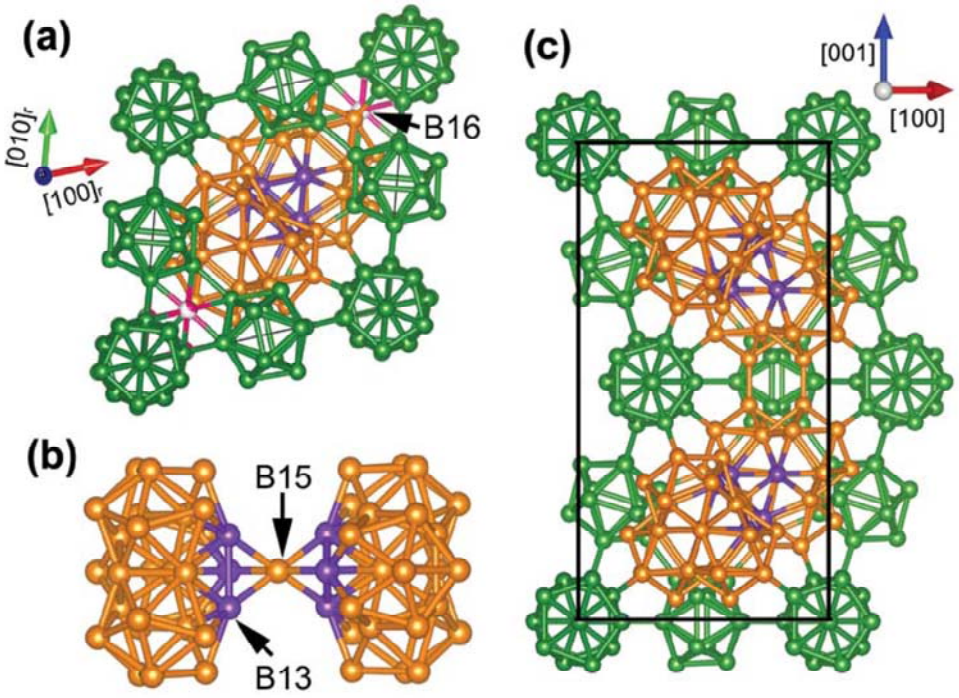

Figure 1. (a) Structure of β-B_{105} with the partial occupation site B16 shown with half red half white ball, viewed along $[001]_r$ direction.
(b) The B_{28}-B-B_{28} unit in the β-B crystal structure. The B_{28} units are represented by orange balls. The B13 site is represented by the purple balls. Fig (b) is part of (a) rotated to (011) plane.
(c) Structure of the new τ-B_{105} phase, view along [010] direction.

Figure 2

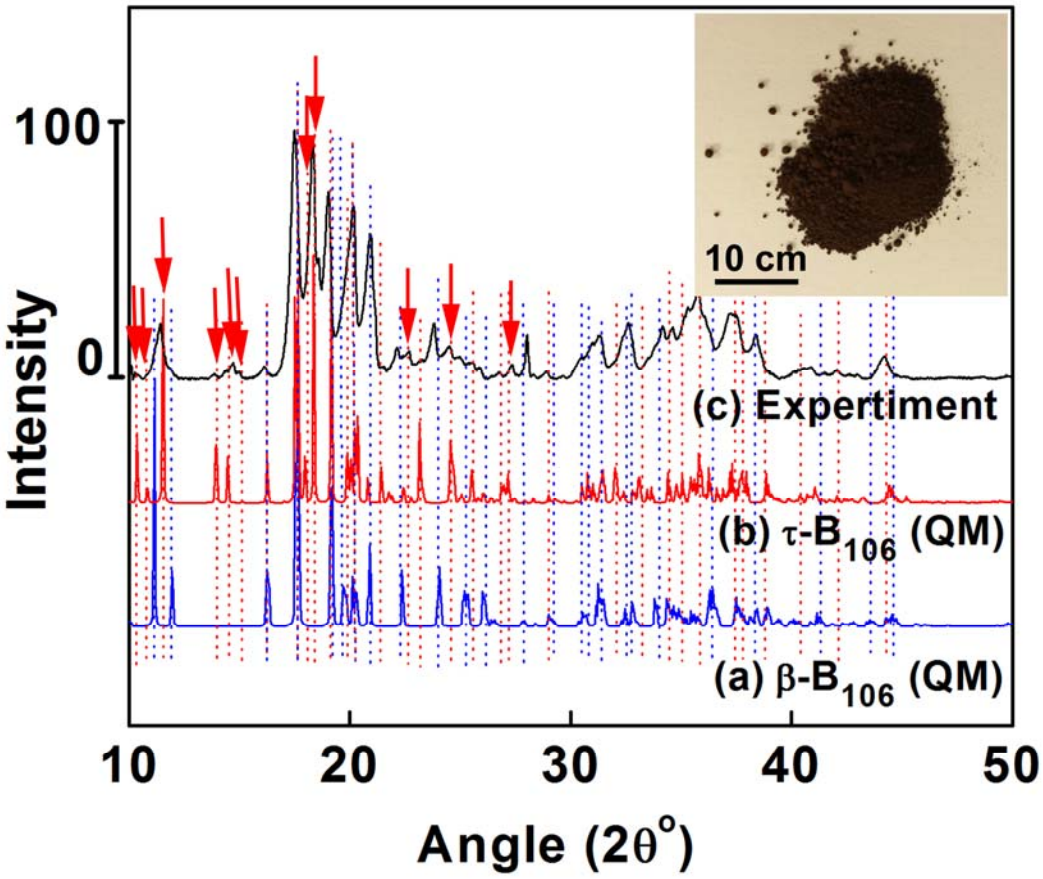

Figure 2. Experimental X-ray diffraction scan compared with simulated patterns based on QM calculations. The phases identified from the powders were found to be a combination of rhombohedral β-B (blue) and τ-B (red) phases indicating with the dotted lines. The insert shows the boron powder.

Figure 3

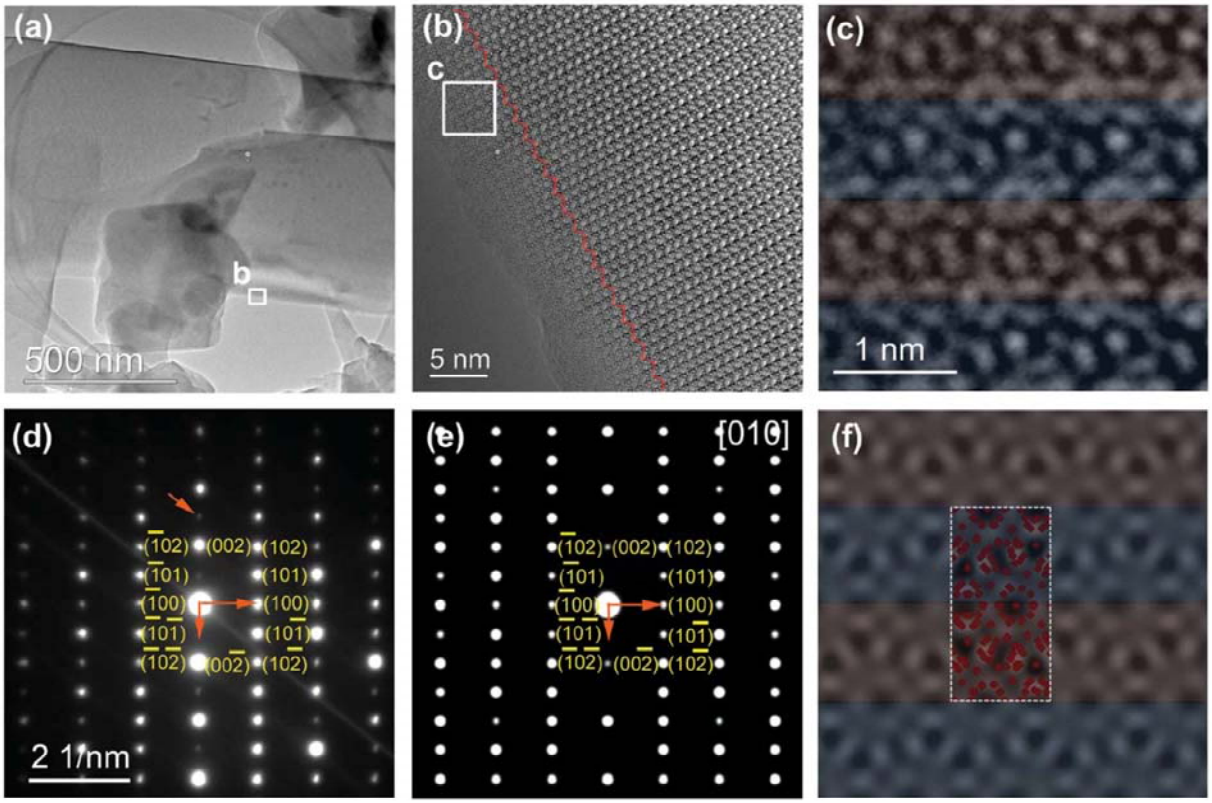

Figure 3. TEM characterization of τ-B_{106}. (a**)** A typical low magnification TEM image showing the powder morphology. (b) Higher magnification TEM images of the boron structure viewed along the [010] zone axis. (c**)** Experimental high resolution TEM image. The mirror symmetry or twinning was observed to repeat perfectly for every other layer of the β-B unit cell in the real space image. (d**)** A SAED pattern recorded for the region imaged in **b** and indexed to be the τ-B_{106} structure. (e) The calculated SAED of the QM predicted τ-B_{106} structure, projected along the [010] orientation. The relative intensity of spots in SAED is highly dependent on foil thickness, precise orientation, *etc.*. (f) The simulated HRTEM image calculated using the QM predicted τ-B_{106} structure. This matches the experimental image and demonstrates the mirror symmetry for the alternating unit cell of τ-B_{106}. The reflections associated with the matrix and the twin are highlighted and indexed in (d). The unit cell for τ-B consists of 212 atoms and the atom positions (red) are overlaid on the simulated image in (f).

Table 1. Energy of various boron phases relative to the α-B_{12} phase.

Structure	α-B_{12}	β-B_{106}	τ-B_{106}	γ-B_{28}
Energy without ZPE correction (meV/atom)	0	1.1	-12.7	27.3
Energy with ZPE correction (meV/atom)	0	-2.3	-16.1	−
Energy with ZPE and dispersion correction (meV/atom)	0	4.3	-9.5	−